JACS
JOURNAL OF THE AMERICAN CHEMICAL SOCIETY
Article
pubs.acs.org/JACS

Layered Hybrid Perovskites with Micropores Created by Alkylammonium Functional Silsesquioxane Interlayers

Sho Kataoka,* Subhabrata Banerjee, Akiko Kawai, Yoshihiro Kamimura, Jun-Chul Choi, Tetsuya Kodaira, Kazuhiko Sato, and Akira Endo*

National Institute of Advanced Industrial Science and Technology (AIST), 1-1-1 Higashi, Tsukuba, Ibaraki 305-8565, Japan

Supporting Information

ABSTRACT: Layered organic–inorganic hybrid perovskites that consist of metal halides and organic interlayers are a class of low-dimensional materials. Here, we report the fabrication of layered hybrid perovskites using metal halides and silsesquioxane with a cage-like structure. We used a silsesquioxane as an interlayer to produce a rigid structure and improve the functionality of perovskite layers. Propylammonium-functionalized silsesquioxane and metal halide salts ($CuCl_2$, $PdCl_2$, $PbCl_2$, and $MnCl_2$) were self-assembled to form rigid layered perovskite structures with high crystallinity. The rigid silsesquioxane structure produces micropores between the perovskite layers that can potentially be filled with different molecules to tune the dielectric constants of the interlayers. The obtained silsesquioxane–metal halide hybrid perovskites exhibit some characteristic properties of layered perovskites including magnetic ordering ($CuCl_4^{2-}$ and $MnCl_4^{2-}$) and excitonic absorption/emission ($PbCl_4^{2-}$). Our results indicate that inserting silsesquioxane interlayers into hybrid perovskites retains and enhances the low-dimensional properties of the materials.

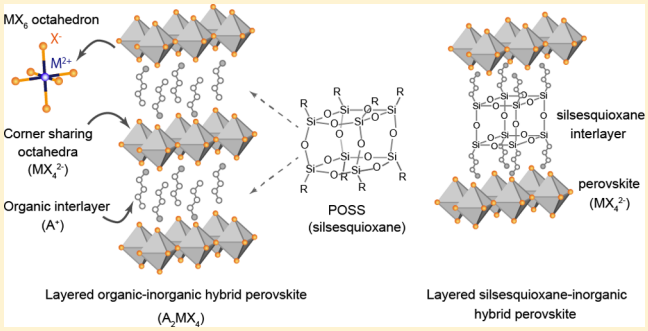

INTRODUCTION

Organic–metal halide hybrid perovskites have recently attracted particular attention in the fields of semiconductors,[1−3] solar cells,[4−8] optics,[3,9] scintillators,[10] and ferromagnets.[11−14] Generally, metal halide perovskites are separated by alkylammonium cations that act as a barrier preventing magnetic and electronic coupling.[12,15] These materials are also low-dimensional compounds and exhibit unique features that differ from those of the original perovskites. As a class of low-dimensional perovskites, A_2MX_4-type layered perovskites contain alternate sheets of alkylammonium cations (A^+) and MX_4^{2-} octahedra (M, bivalent metal; X, halogen atom), as shown in Figure 1. A_2MX_4-type layered perovskites have been widely investigated over the past few decades.[12,15] Because this well-defined structure is easily prepared by soft chemical methods, many organic cations have been used to tailor such materials for various applications.[12,15,16] These studies revealed that properties of the organic cations such as size, electronic excited states, and dielectric constant alter the performance of layered perovskites.[17,18]

Silsesquioxanes are siloxane compounds with the composition formula, $(RSiO_{3/2})_n$, where one silicon atom is connected to three oxygen atoms and one organic moiety, R, to form a T unit.[19] When n = 8, the silsesquioxane can have a cubic cage-like structure with eight functional groups (Figure 1).[19,20] This unique silsesquioxane structure is also referred to as a polyhedral oligomeric silsesquioxane (POSS). Importantly, POSSs possess both the robust properties of silica and the flexible properties of organic compounds. A number of organic functionalized POSSs have been reported and are recognized as versatile organic–inorganic hybrid materials.[20] The addition of POSSs to products can improve their original mechanical and thermal properties as well as chemical stability, miscibility, and rigidity. For example, POSSs are sometimes grafted onto

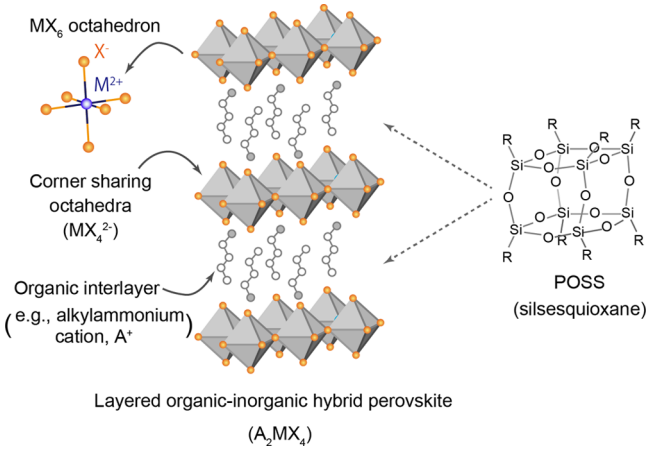

Figure 1. Schematic diagram of layered organic–inorganic hybrid perovskites and POSS.

Received: January 10, 2015
Published: March 16, 2015

DOI: 10.1021/jacs.5b00290
J. Am. Chem. Soc. 2015, 137, 4158–4163

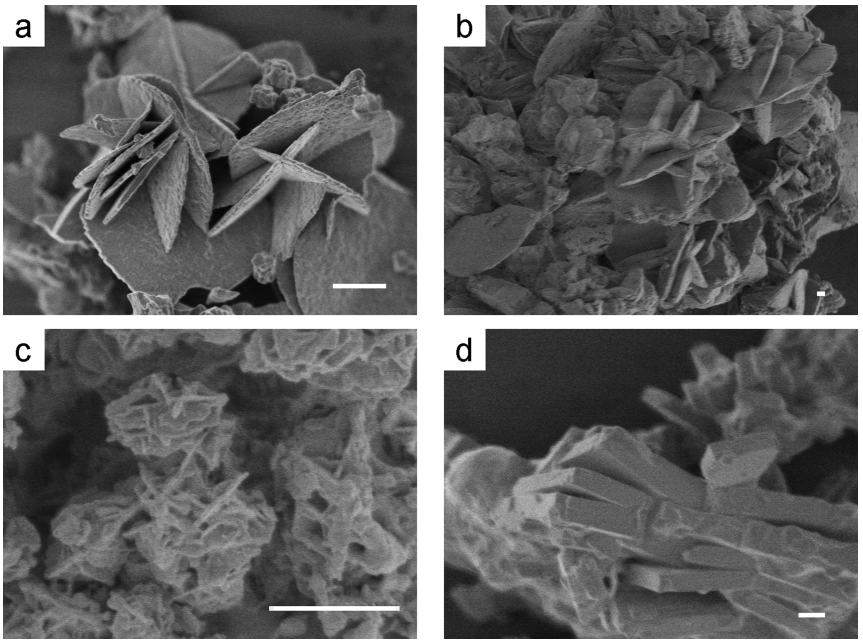

Figure 2. FE-SEM images of the silsesquioxane–metal halide complexes: (a) CuPOSS, (b) PdPOSS, (c) PbPOSS, and (d) MnPOSS (scale bar: 1 μm).

organic polymers to increase crystallinity because of their rigidity.[21] POSSs have also been added to electrical and thermal insulators because of their miscibility.[22,23] These applications suggest that POSSs are potentially suitable as an interlayer in layered materials. If a POSS is inserted between layered perovskites, it may enhance their properties and functionality. To date, complexes of POSS and metal halides or metals have been reported,[24−26] and the formation of random siloxane networks between perovskite layers has been attempted.[27,28] However, this report presents a completely different approach. We form layered POSS–metal halide hybrid perovskites using a propylammonium-functionalized POSS (A–POSS) and several metal halides under ambient conditions and then evaluate the physical properties of the resultant layered perovskites.

EXPERIMENTAL SECTION

Materials. All chemicals were used as received. Ethanol, methanol, 2-propanol, acetone, dimethyl sulfoxide, ethylene glycol, hydrochloric acid (HCl), copper(II) chloride, 2-hydrate ($CuCl_2$), palladium chloride ($PdCl_2$), lead chloride ($PbCl_2$), and manganese(II) chloride, 4-hydrate ($MnCl_2$) were purchased from Kishida Chemical Co. (Osaka, Japan). 3-Aminopropyltriethoxysilane (APTES) was purchased from Shin-Etsu Chemical Co., Ltd. (Tokyo, Japan). Water used in experiments was prepared using a Milli-Q Ultrapure Water System (Direct-Q, Millipore, Billerica, MA).

Preparation of POSS-Metal Halide Complexes. Propylammonium silsesquioxane (A–POSS) was synthesized using a reported method.[29−31] Briefly, a mixture of APTES (30 mL), HCl (41 mL), and MeOH (240 mL) was stirred for 5 h and then left to stand at room temperature for 5–14 days. After a white precipitate formed, it was collected by filtration and washed with cold methanol to give A–POSS (approximately 5 g). A–POSS and metal halides ($CuCl_2$, $PdCl_2$, $PbCl_2$ and $MnCl_2$) were first dissolved in aqueous hydrochloric acid or water, and then complexes were precipitated as microcrystalline precipitates by adding the mixture to poor solvents. Hereafter, the obtained complexes are referred to as CuPOSS, PdPOSS, PbPOSS, and MnPOSS. Detailed synthetic procedures are described in the Supporting Information.

Characterization of POSS–Metal Halide Complexes. Field-emission scanning electron microscope (FE-SEM) images of the complexes were observed using an FE-SEM (S-4800, Hitachi High-Technologies, Japan) at an accelerating voltage of 0.7–1.0 kV without any metal coating. ^{29}Si solid-state NMR spectra were recorded at 12.5 kHz using an NMR spectrometer (AVANCE-400, Bruker, Billerica, MA) equipped with a magic-angle spinning (MAS) probe. Powder samples were transferred to standard 4-mm zirconia rotors for NMR measurements. Powder X-ray diffraction (XRD) patterns of the complexes were collected using an X-ray diffractometer (D8 Advance, Bruker) with Cu Kα radiation (λ = 0.15406 nm, 40 kV, 40 mA). Nitrogen (N_2) sorption isotherms were measured at 77 K using an adsorption apparatus (Belsorp-mini, BEL Japan Inc.). Specific surface areas were calculated using Brunauer–Emmett–Teller (BET) theory. Supplemental elemental analyses of CuPOSS were performed using an ion chromatograph (Dionex ICS-2000, Thermo Fisher Scientific, Inc., Waltham, MA) equipped with an automatic quick furnace (AQF-100, Mitsubishi Chemical Co., Japan) and an inductively coupled plasma atomic emission spectrometer (ICP-AES: SPS-7800, SII Nanotechnology, Inc., Japan).

Magnetic moments of CuPOSS and MnPOSS were measured using a superconducting quantum interference device (SQUID: MPMS-5s: Quantum Design, Inc., San Diego, CA) equipped with a reciprocating sample option system. Optical properties of PbPOSS were analyzed using powdered samples on glass slides. Diffuse reflectance UV–vis absorption spectra were measured using a UV–vis spectrophotometer (UV-2600, Shimadzu, Japan) and photoluminescence spectra were obtained by excitation at 320 nm using a spectrofluorometer (FluoroMax-4, Horiba, Japan) equipped with a Xe lamp.

RESULTS AND DISCUSSION

The silsesquioxane–metal halide complexes were characterized to confirm their structures. First, FE-SEM images of the powdered complexes were obtained (Figure 2). All the complexes consist of thin plates. CuPOSS and PdPOSS samples contained particularly thin disk-like shapes with sharp edges (Figure 2a,b), while the plates of PbPOSS are less defined (Figure 2c). MnPOSS clearly consists of thick rectangular plates (Figure 2d). In contrast, A–POSS did not form plates, and its complexes with $ZnCl_2$ and $CoCl_2$ exhibited a rod-like morphology (see Figure S1 in the Supporting Information). The morphology of these complexes is

DOI: 10.1021/jacs.5b00290
J. Am. Chem. Soc. 2015, 137, 4158−4163

determined during the precipitation process and is specific to the metal halide used. This indicates that the observed plate-like morphology presumably originates from their layered crystal structures.[32]

Solid-state ^{29}Si MAS NMR spectra were recorded for the complexes and A–POSS (Figure 3). A–POSS exhibited one

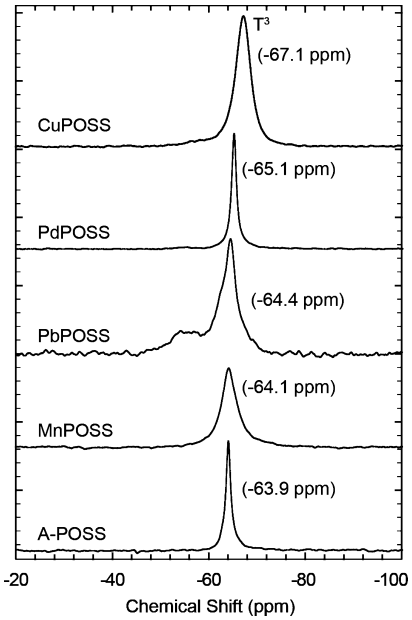

Figure 3. Solid-state ^{29}Si MAS NMR spectra of the obtained complexes and A–POSS.

sharp peak centered at δ_{Si} = −63.9 ppm that is attributed to a T^3 peak,[29−31,33,34] which is evidence for the presence of a cubic cage-like structure as shown in Figure 1. All of the complexes exhibited only one sharp peak similar to A–POSS (δ_{Si} = −67.1 ppm for CuPOSS; δ_{Si} = −65.1 ppm for PdPOSS; δ_{Si} = −64.4 ppm for PbPOSS; δ_{Si} = −64.1 ppm for MnPOSS). These results confirm that the cage structure of A–POSS remains intact in the complexes with metal halides. The peaks observed for CuPOSS and MnPOSS are slightly broadened, which is presumably because of the magnetic properties of these metal halide layers. For PbPOSS, the main peak is slightly broadened and is accompanied by a small band around δ_{Si} = −55 ppm. This band may arise from partial degradation of POSS moieties during synthesis.

Powder XRD patterns of the complexes contain sharp peaks, which is clear evidence for their high crystallinity (Figure 4). The narrow peaks (indicated by *) that appear at equal increments (2θ = 5°) are characteristic of 00*l* type reflections of layered compounds. The corresponding layer distance calculated from Bragg's law is 1.76 nm for CuPOSS, 1.70 nm for PdPOSS, 1.61 nm for PbPOSS, and 1.74 nm for MnPOSS. These diffraction patterns closely resemble those of reported layered perovskites,[35−37] but differ substantially from that of A–POSS. More importantly, these layer distances approximately correspond to the size of A–POSS (approximately 1.4 nm).[24] Therefore, the FE–SEM, NMR, and XRD results lead us to conclude that the obtained silsesquioxane–metal halide complexes form layered perovskite structures. We also conducted elemental analyses of CuPOSS using ion chromatography for the Cl species and ICP-AES for the Cu and Si species. The calculated chemical formula of CuPOSS is

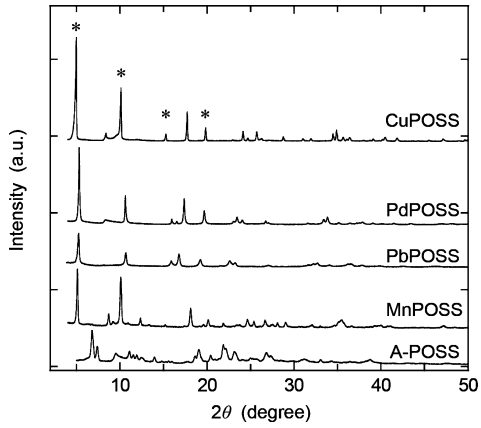

Figure 4. Powder XRD patterns obtained for silsesquioxane–metal halide complexes: asterisk (*) indicates 00*l* type reflections.

$[Si_8O_{12}(C_3H_6NH_3)_8][CuCl_4]_4$, which is in good agreement with the formation of a layered perovskite. Furthermore, we obtained a preliminary single-crystal X-ray diffraction result for CuPOSS (Figure S2 in the Supporting Information). This result also implies the formation of a layered copper chloride structure, which is consistent with our other results.

One unique characteristic of these silsesquioxane–metal halide hybrid perovskites is their porous structure. N_2 sorption isotherms were obtained for the layered perovskites and A–POSS (Figure 5a). A–POSS did not adsorb N_2, which supports the assertion that N_2 molecules cannot enter the POSS cage.[38] In contrast, CuPOSS and PdPOSS exhibit type-I N_2 sorption isotherms, indicating the presence of micropores with diameters less than 2 nm in these compounds. The amount of N_2 adsorbed at P/P_0 = 0.95 is approximately 70 mL-STP g^{-1}, which is equivalent to nearly five N_2 molecules adsorbed per one POSS cage. The BET specific surface areas calculated for CuPOSS and PdPOSS were 205 and 187 m^2/g, respectively. In addition, N_2 molecules were adsorbed into the micropores of MnPOSS (see Figure S3 in the Supporting Information). However, PbPOSS did not readily adsorb N_2 (Figure 5a). These results suggest that N_2 molecules were adsorbed onto the surface of the POSS cage between the perovskite layers in all of the complexes except PbPOSS (Figure 5b). The microporous structure formed presumably because of the size and rigidity of A–POSS as a well-defined interlayer with a distance of 1.70–1.76 nm. The results indicate that an open space exists between the perovskite layers in all of the complexes except PbPOSS. Filling this space with target compounds may allow the properties of the interlayers to be easily tuned.

The physical properties of the obtained complexes were then measured to evaluate the role of A–POSS as an interlayer. First, the temperature dependence of the molar susceptibility, χ_{mol}, of CuPOSS was measured from 50 to 2 K at 0.5 Oe using a SQUID. When the temperature was less than 10 K, χ_{mol} abruptly increased, indicating the presence of ferromagnetic ordering in CuPOSS (Figure 6a). The Weiss constant (T_w) was determined by fitting the $1/\chi_{mol}$ data above 22 K to the Curie–Weiss law:

$$\frac{1}{\chi_{mol}} = \frac{1}{c}(T - T_w)$$

giving T_w = 18 K, which is also consistent with our argument (see the inset in Figure 6a). In addition, the maximum

DOI: 10.1021/jacs.5b00290
J. Am. Chem. Soc. 2015, 137, 4158–4163

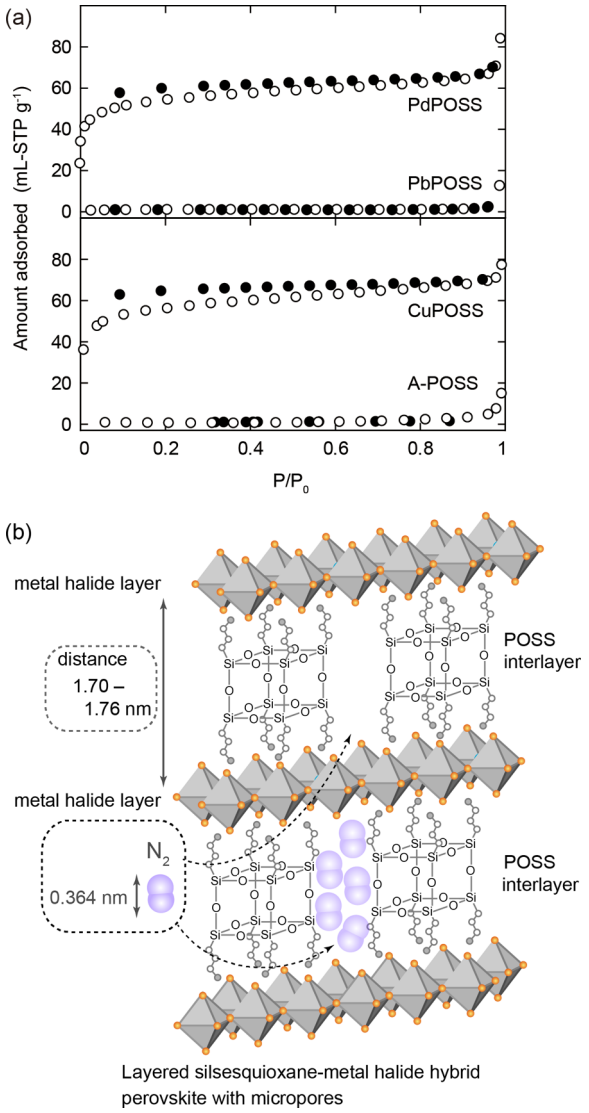

Figure 5. (a) N_2 sorption isotherms of silsesquioxane–metal halide complexes at 77 K (open circles, adsorption; filled circles, desorption). (b) Schematic diagram of layered POSS–inorganic hybrid perovskites with N_2 adsorbed between layers.

susceptibility is around 5 K, which is slightly different from previous reports for layered copper chloride perovskites where no maximum was observed.[39,40] The same phenomenon was also observed at 10 Oe (data not shown). We were unable to fully interpret the χ_{mol} data for CuPOSS measured at less than 5 K. For comparison, the temperature dependence of the molar susceptibility of MnPOSS was also measured from 2 to 40 K at 0.5 Oe with heating after zero field cooling (Figure 6a). χ_{mol} for MnPOSS remained small even at low temperatures, compared with that for CuPOSS. By fitting the $1/\chi_{mol}$ data above 22 K, T_w for MnPOSS was estimated to be −39 K (see the inset in Figure 6a). These results are indicative of an antiferromagnetic interaction between Mn^{2+} ions in MnPOSS.[41]

The magnetic moments of CuPOSS were recorded in a field ranging from 0 to 50 kOe at 2 K (Figure 6b). The magnetic moment of CuPOSS rapidly increases in a small magnetic field, which supports the presence of ferromagnetic ordering.[39] The saturation magnetization of CuPOSS is 0.95 μ_B/each which is almost the same as the literature value for a layered perovskite with a similar structure of 1.06 μ_B/each.[39] The hysteresis loop

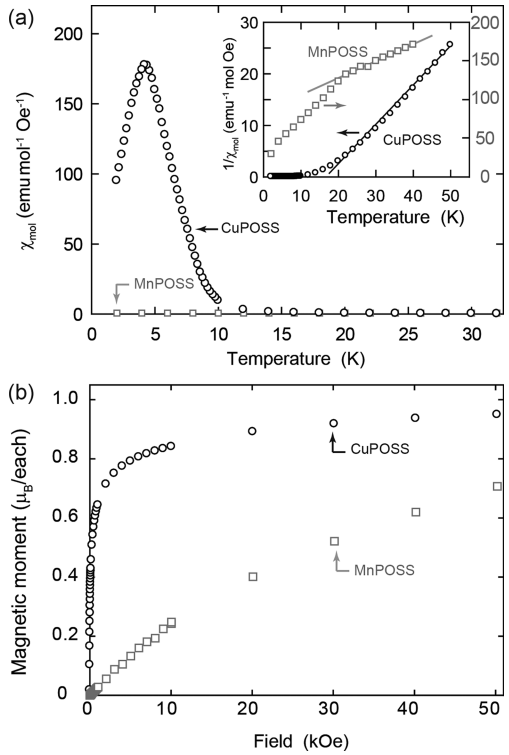

Figure 6. Magnetic properties of CuPOSS (circles) and MnPOSS (squares). (a) Temperature dependence of molar susceptibility, χ_{mol} at 0.5 Oe. (Inset) Plot of $1/\chi_{mol}$–T. (b) Isothermal magnetic moment measurements from 0 to 50 kOe.

and remnant magnetization of CuPOSS are small (data not shown). The field dependence of the magnetic moments of MnPOSS was also recorded in a field ranging from 0 to 50 kOe at 2 K. The magnetic moments were nearly proportional to the applied field, which is markedly different behavior from CuPOSS. To prove the presence of an antiferromagnetic interaction in MnPOSS, further investigation is required. Nonetheless, both CuPOSS and MnPOSS exhibit some magnetic ordering features in their perovskite layers. This suggests that POSS serves as an effective interlayer, similar to other alkylammonium compounds.

UV–vis absorption and photoluminescence emission spectra of powder PbPOSS were measured at room temperature (Figure 7). The diffuse reflectance UV–vis spectrum of

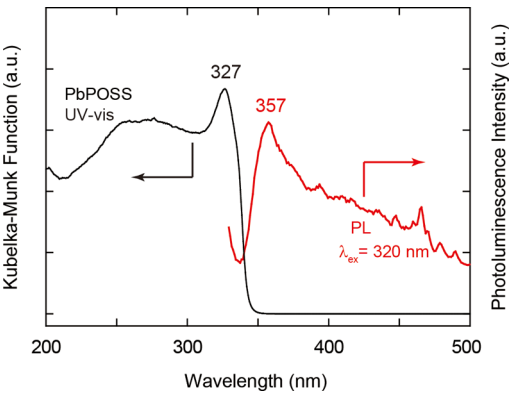

Figure 7. Diffuse reflectance UV–vis absorption and photoluminescence emission (λ_{ex} = 320 nm) spectra for PbPOSS.

DOI: 10.1021/jacs.5b00290
J. Am. Chem. Soc. 2015, 137, 4158–4163

PbPOSS exhibits a sharp, intense absorption peak at 327 nm along with broad shoulder bands similar to those of reported layered perovskites containing lead halides at around 330 nm.[27,42−44] The photoluminescence spectrum obtained upon excitation at 320 nm contains a strong, sharp emission peak at 357 nm. Small peaks from 450 to 470 nm in the spectrum originate from the Xe lamp. The emission peak of PbPOSS at 357 nm is slightly higher than that at around 340 nm in other reports.[27,42,44] Nevertheless, the strong, sharp peaks exhibited by PbPOSS are typical features of excitonic absorption and emission,[1,3,9,27,28] which indicates the presence of stable excited electron−hole pairs (i.e., excitons) in the $PbCl_4^{2-}$ layers. Therefore, the silsesquioxane interlayers can stabilize excitons in the perovskite layers of PbPOSS in the same way as alkylammonium compounds.

■ CONCLUSIONS

In this study, we fabricated layered hybrid perovskites consisting of a POSS and metal halides. The layered hybrid perovskites contained micropores and some exhibited magnetic ordering (CuPOSS and MnPOSS) and excitonic absorption/emission (PbPOSS). The micropores between the metal halide perovskite layers that were formed by POSS may open new avenues of research into controlling the properties of perovskites by filling with various molecules.

■ ASSOCIATED CONTENT

Supporting Information

Detailed synthetic procedures for POSS−metal halide complexes; additional POSS−metal halide complexes containing $ZnCl_2$ and $CoCl_2$; single-crystal X-ray diffraction data; additional N_2 sorption data for MnPOSS; additional thermal gravimetric analyses. This material is available free of charge via the Internet at http://pubs.acs.org.

■ AUTHOR INFORMATION

Corresponding Authors

*s-kataoka@aist.go.jp
*endo-akira@aist.go.jp

Notes

The authors declare no competing financial interest.

■ ACKNOWLEDGMENTS

This work was fully supported by the "Development of Innovative Catalytic Processes for Organosilicon Functional Materials" project from the New Energy and Industrial Technology Development Organization (NEDO). We are especially grateful to Drs. Norihisa Fukaya, Toshiaki Taira, and Noriyuki Takada (AIST) for fruitful discussions. We also thank Drs. Yasutaka Kuwahara, Toshikazu Takahashi, and Kunio Suzuki (AIST), and Mr. Susumu Mimura (Horiba Ltd., Japan) for their assistance with UV−vis, solid-state NMR, FE-SEM, and photoluminescence measurements. SQUID measurements were performed in Nano-Processing Facility (NPF) at AIST. We acknowledge Drs. Teruhisa Ootsuka and Masashi Yamazaki (NPF) for their generous assistance during SQUID measurements.

■ REFERENCES

(1) Ishihara, T.; Takahashi, J.; Goto, T. *Solid State Commun.* **1989**, *69*, 933.
(2) Kagan, C. R.; Mitzi, D. B.; Dimitrakopoulos, C. D. *Science* **1999**, *286*, 945.
(3) Tanaka, K.; Sano, F.; Takahashi, T.; Kondo, T.; Ito, R.; Ema, K. *Solid State Commun.* **2002**, *122*, 249.
(4) Kojima, A.; Teshima, K.; Shirai, Y.; Miyasaka, T. *J. Am. Chem. Soc.* **2009**, *131*, 6050.
(5) Lee, M. M.; Teuscher, J.; Miyasaka, T.; Murakami, T. N.; Snaith, H. J. *Science* **2012**, *338*, 643.
(6) Hao, F.; Stoumpos, C. C.; Duyen Hanh, C.; Chang, R. P. H.; Kanatzidis, M. G. *Nat. Photonics* **2014**, *8*, 489.
(7) Jeon, N. J.; Noh, J. H.; Kim, Y. C.; Yang, W. S.; Ryu, S.; Seok, S. I. *Nat. Mater.* **2014**, *13*, 897.
(8) Smith, I. C.; Hoke, E. T.; Solis-Ibarra, D.; McGehee, M. D.; Karunadasa, H. I. *Angew. Chem., Int. Ed.* **2014**, *53*, 11232.
(9) Kitazawa, N. *J. Mater. Sci.* **1998**, *33*, 1441.
(10) Shibuya, K.; Koshimizu, M.; Takeoka, Y.; Asai, K. *Nucl. Instrum. Methods Phys. Res., Sect. B* **2002**, *194*, 207.
(11) Estes, W. E.; Losee, D. B.; Hatfield, W. E. *J. Chem. Phys.* **1980**, *72*, 630.
(12) Mitzi, D. B. In *Progress in Inorganic Chemistry*; Karlin, K. D., Ed.; Wiley: New York, 1999; Vol. *48*, p 1.
(13) Akhtar, N.; Polyakov, A. O.; Aqeel, A.; Gordiichuk, P.; Blake, G. R.; Baas, J.; Amenitsch, H.; Herrmann, A.; Rudolf, P.; Palstra, T. T. *Small* **2014**, *10*, 4912.
(14) Willett, R.; Place, H.; Middleton, M. *J. Am. Chem. Soc.* **1988**, *110*, 8639.
(15) Cheng, Z.; Lin, J. *CrystEngComm* **2010**, *12*, 2646.
(16) Kikuchi, K.; Takeoka, Y.; Rikukawa, M.; Sanui, K. *Colloids Surf., A* **2005**, *257−58*, 199.
(17) Braun, M.; Tuffentsammer, W.; Wachtel, H.; Wolf, H. C. *Chem. Phys. Lett.* **1999**, *303*, 157.
(18) Tanaka, K.; Kondo, T. *Sci. Technol. Adv. Mater.* **2003**, *4*, 599.
(19) Baney, R. H.; Itoh, M.; Sakakibara, A.; Suzuki, T. *Chem. Rev.* **1995**, *95*, 1409.
(20) Cordes, D. B.; Lickiss, P. D.; Rataboul, F. *Chem. Rev.* **2010**, *110*, 2081.
(21) Carroll, J. B.; Waddon, A. J.; Nakade, H.; Rotello, V. M. *Macromolecules* **2003**, *36*, 6289.
(22) Bocek, J.; Matejka, L.; Mentlik, V.; Trnka, P.; Slouf, M. *Eur. Polym. J.* **2011**, *47*, 861.
(23) Dasari, A.; Yu, Z.-Z.; Mai, Y.-W.; Cai, G.; Song, H. *Polymer* **2009**, *50*, 1577.
(24) Goodgame, D. M. L.; Kealey, S.; Lickiss, P. D.; White, A. J. P. *J. Mol. Struct.* **2008**, *890*, 232.
(25) do Carmo, D. R.; Paim, L. L.; Metzker, G.; Dias Filho, N. L.; Stradiotto, N. R. *Mater. Res. Bull.* **2010**, *45*, 1263.
(26) Naka, K.; Fujita, M.; Tanaka, K.; Chujo, Y. *Langmuir* **2007**, *23*, 9057.
(27) Cheng, Z. Y.; Gao, B. X.; Pang, M. L.; Wang, S. Y.; Han, Y. C.; Lin, J. *Chem. Mater.* **2003**, *15*, 4705.
(28) Cheng, Z.-Y.; Shi, B.-L.; Gao, B.-X.; Pang, M.-L.; Wang, S.-Y.; Han, Y.-C.; Lin, J. *Eur. J. Inorg. Chem.* **2005**, *2005*, 218.
(29) Tanaka, K.; Inafuku, K.; Adachi, S.; Chujo, Y. *Macromolecules* **2009**, *42*, 3489.
(30) Feher, F. J.; Wyndham, K. D. *Chem. Commun.* **1998**, 323.
(31) Gravel, M. C.; Zhang, C.; Dinderman, M.; Laine, R. M. *Appl. Organomet. Chem.* **1999**, *13*, 329.
(32) Ahari, H.; Bedard, R. L.; Bowes, C. L.; Coombs, N.; Dag, O.; Jiang, T.; Ozin, G. A.; Petrov, S.; Sokolov, I.; Verma, A.; Vovk, G.; Young, D. *Nature* **1997**, *388*, 857.
(33) Kaneko, Y.; Shoiriki, M.; Mizumo, T. *J. Mater. Chem.* **2012**, *22*, 14475.
(34) Oviatt, H. W.; Shea, K. J.; Small, J. H. *Chem. Mater.* **1993**, *5*, 943.
(35) Mitzi, D. B.; Liang, K. N. *Chem. Mater.* **1997**, *9*, 2990.
(36) Xiao, Z.-L.; Chen, H.-Z.; Shi, M.-M.; Wu, G.; Zhou, R.-J.; Yang, Z.-S.; Wang, M.; Tang, B.-Z. *Mater. Sci. Eng., B* **2005**, *117*, 313.
(37) Liang, K. N.; Mitzi, D. B.; Prikas, M. T. *Chem. Mater.* **1998**, *10*, 403.

DOI: 10.1021/jacs.5b00290
J. Am. Chem. Soc. 2015, 137, 4158−4163

(38) Zhang, C. X.; Babonneau, F.; Bonhomme, C.; Laine, R. M.; Soles, C. L.; Hristov, H. A.; Yee, A. F. *J. Am. Chem. Soc.* **1998**, *120*, 8380.
(39) Willett, R. D.; Gomez-Garcia, C. J.; Twamley, B. *Eur. J. Inorg. Chem.* **2012**, 3342.
(40) Zhou, P.; Drumheller, J. E. *J. Appl. Phys.* **1990**, *67*, 5755.
(41) Zhang, Z. J.; Xiang, S. C.; Zhang, Y. F.; Wu, A. Q.; Cai, L. Z.; Guo, G. C.; Huang, J. S. *Inorg. Chem.* **2006**, *45*, 1972.
(42) Papavassiliou, G. C.; Koutselas, I. R. *Synth. Met.* **1995**, *71*, 1713.
(43) Era, M.; Maeda, K.; Tsutsui, T. *Thin Solid Films* **1998**, *331*, 285.
(44) Papavassiliou, G. C.; Mousdis, G. A.; Koutselas, I. B. *Adv. Mater. Opt. Electron.* **1999**, *9*, 265.

DOI: 10.1021/jacs.5b00290
J. Am. Chem. Soc. 2015, 137, 4158−4163